Electronic Supplementary Material (ESI) for Physical Chemistry Chemical Physics.

Electronic Supplementary Information

Graphene Oxide Inhibits hIAPP Amyloid Fibrillation and Toxicity in Insulin-Producing NIT-1 Cells

Praveen Nedumpully-Govindan,[1] Esteban N. Gurzov,[2,3] Pengyu Chen,[4] Emily H. Pilkington,[5] William J. Stanley,[2,3] Sara A. Litwak,[2] Thomas P. Davis,[5,6] Pu Chun Ke[5] and Feng Ding[1*]*

[1]Department of Physics and Astronomy, Clemson University, Clemson, SC 29634, USA
[2]St Vincent's Institute of Medical Research, 9 Princes Street, Fitzroy, VIC 3065, Australia
[3]Department of Medicine, St. Vincent's Hospital, The University of Melbourne, Melbourne, Australia
[4]Department of Mechanical Engineering, University of Michigan, Ann Arbor, MI, 28109, USA
[5]ARC Center of Excellence in Convergent Bio-Nano Science and Technology, Monash Institute of Pharmaceutical Sciences, Monash University, 381 Royal Parade, Parkville, VIC 3052, Australia
[6]Department of Chemistry, University of Warwick, Gibbet Hill, Coventry, CV4 7AL, United Kingdom

[*] Address correspondence to:
Feng Ding: fding@clemson.edu, and Pu Chun Ke: pu-chun.ke@monash.edu.

Contents:

Supplementary Experimental and Computational Methods

Supplementary Figures S1-S3

Experimental and Computational Methods

Sample Preparations: Human islet amyloid polypeptide (hIAPP) (KCNTATCATQRLANFLVHSSNNFGAILSSTNVGSNTY; Modifications: Tyr-37=C-terminal amide, disulfide bridge: 2-7; purity: >95%; MW: 3,906) was obtained from Abcam in lyophilized powder form. The water solubility of the hIAPP was 5 mg/mL. For experiments the hIAPP was weighed on a Cubis MSE balance (Sartorius, 0.01 mg resolution) and dissolved in Milli-Q water to form a 0.25 mg/mL (64 μM) stock solution immediately prior to the measurements. GO stock of 2 mg/mL in water was acquired from Sigma. The dimensions of the GO were characterized by TEM (Fig. 1A) and chemical compositions of the nanosheets were analyzed by XRD as pre-described[1], showing the main elements of carbon and oxygen (atomic percentage to total carbon: 46.7%), and trace amounts of sulfur (atomic percentage to total carbon: 2%) and manganese (0.5%).

Zeta Potential: The zeta potentials of hIAPP (64 μM) and GO (0.1 mg/mL) in Milli-Q water were determined using a DLS device (Zetasizer Nano S90, Malvern Instruments) at room temperature.

TEM: Copper grids (300-mesh, carbon coated) were glow-discharged in nitrogen to promote hydrophilicity. Aqueous hIAPP (0.1 mg/mL or 26 μM), GO (0.1 mg/mL), and a mixture of hIAPP-GO of equal volume, all incubated overnight at 4°C, were pipetted onto the grids and allowed 20s of adsorption. Excess samples were then drawn off using filter paper and the grids washed using Milli-Q water. Staining was undertaken using 2% uranyl acetate for 20s, with excess stain drawn off. The grids were dried under heated airflow for 20-30s. The samples were then examined using a Tecnai G2 F30 Transmission Electron Microscope (FEI, Eindhoven, The Netherlands) operating at a voltage of 300 kV. Images were recorded using an UltraScan 1000

CCD camera (2k×2k, Gatan, California, USA).

Raman spectroscopy: Raman spectroscopy was undertaken using an inVia confocal Raman microscope (Renishaw). GO, hIAPP (both at 0.25 mg/mL) and GO-hIAPP mixed at 1:1 and 1:5 weight ratios in aqueous solution were excited by a laser line at 785 nm, with a power of 500 mW. Sample spectra were generated with in-built WiRE 2.0 software and peaks fitted with PeakFit (Systat) using Gaussian-Lorentzian modelling.

Circular Dichroism Spectroscopy: Spectra of the secondary structure of hIAPP (0.1 mg/mL) and hIAPP in the presence of GO (0.1 mg/mL) were recorded using a J-815 circular dichroism spectrometer (JASCO), using a quartz cuvette of 3 mm path length for the wavelength range of 195~300 nm at room temperature. Data were collected every 0.1 nm at a scanning speed of 50 nm/min and averaged over three measurements. The protein samples were incubated with GO for 4 h at room temperature prior to each measurement. The final spectra were baseline-corrected and the data were measured in mean residue ellipticity (θ) and converted to standard unit of $deg \cdot cm^2 dmol^{-1}$ using equation $[\theta]=(\theta \times M_0)/(10{,}000 \times C_{soln} \times L)$, where M_0 denotes the mean residue molecular weight (114 g/mol), C_{soln} is the protein concentration (g/mL), and L is the path length through the buffer (cm).

Discrete Molecular Dynamics Simulations: Simulations were carried out using the DMD algorithm, details of which can be found in reference[2]. In short, DMD is a special type of molecular dynamics simulation that uses discretized functions for modeling the inter-atomic potential energy functions. When two atoms encounter a potential step, their velocities change instantaneously following the conservation laws of energy, momentum and angular momentum. The simulation proceeds as a series of such collisions between which atomic velocities remain

constant. This simplification results in an enhanced sampling efficiency of DMD over classical molecular dynamics. We used a united atom representation in which all the heavy atoms and polar hydrogen atoms were explicitly modeled. The potential energy functions in the atomistic DMD simulations include bonded terms representing chemical bonds, bond angles and dihedral angles, and non-bonded terms representing van der Waals, solvation, electrostatic and hydrogen bonding interactions. These parameters for bonded interaction were obtained by statistical analysis of high-resolution structures from protein data bank (PDB). The van der Waals interaction terms were adopted from CHARMM force field[3]. We used the implicit solvent model, EEF1, developed by Lazaridis and Karplus[4]. Electrostatic interactions were calculated between chemical groups with formal charges. Each hIAPP peptide had two charged residues, and our GO model was assumed neutrally charged (see below). The screened electrostatic interactions were modeled by using the Debye–Huckel approximation. The Debye length was set at ~1 nm, assuming a water electric constant of 80, and a monovalent salt concentration of 100 mM.

Simulations Setup: We carried out discrete molecular dynamics (DMD, see below) simulations of hIAPP molecules in the presence and absence of GO nanosheets. For studying the effect of GO on hIAPP–hIAPP interactions and hIAPP aggregation, we simulated systems consisting of one, two, four and six hIAPPs (PDB ID: 2L86[5]). The systems were initialized by placing hIAPP molecules randomly (around the GO nanosheet, when it was present) in the simulation box. All the simulations were carried out in a cubic box of size 100 Å, with periodic boundary condition applied in all directions. GO nanosheet was placed at the center of the box, and carbon atoms of the GO were position restrained to their initial positions. Ten independent copies of each system (with different initial positions and velocities) were carried out for better sampling and to avoid

any bias arising from the initial structure. Each simulated system was energy minimized using steepest descent algorithm for 1000 steps, and DMD simulation was carried out for one million DMD steps (~ 50 ns). During the simulations, the temperature was kept constant at ~ 290 K using Anderson thermostat[6].

Graphene Oxide Structure: We generated honeycomb structure of graphene nanosheets using an in-house builder. Hydroxyl groups and epoxy oxygen atoms were added to about 30% randomly chosen carbon atoms to construct initial our grapheme oxide (GO) model. For studying the effect of surface area on hIAPP aggregation, we prepared GO nanosheet of size 32.6 Å × 38.1 Å. The structure was energy minimized with the Gmolden visualization program[7], using the GAFF force field[8], implemented in Gmolden.

Contact Number Calculations: For estimating hIAPP–GO and hIAPP–hIAPP contact numbers, we calculated the distance between each inter-molecular atom pair. If the distance was equal to or smaller than 5 Å, we considered that as a contact between the two atoms. The contact number between two molecules was then simply defined as the total number of such contacts. The average contact number over the last quarter of each simulation was taken an independent measurement; the error bars in Figs. 3C–D and S3 were estimated using ten independent measurements (from ten independent simulations).

Cell Culture and Viability: The insulin producing NIT-1 cell line was cultured in DMEM (Invitrogen, UK) supplemented with 10% fetal calf serum. The percentage cell death of NIT-1 cells was determined in at least 600 cells per experimental condition by inverted fluorescence microscopy after staining with the DNA dyes Hoechst-33342 (10 μg/mL) and propidium iodide (5 μg/mL). The method utilized here to measure cell viability is quantitative, and has been

validated by systematic comparison against electron microscopy and other well-characterized methods.[9–12] The cells were cultured in Opti-MEM (Life Technologies) for treatment with hIAPP (10 μM), GO (100 μg/mL) or 10 μM hIAPP pre-treated for 16 h with 100 μg/mL GO. hIAPP and GO concentrations were selected according to published data and our own dose response[13]. The cells were treated for 24 h before the viability assessment.

Statistical Analysis: Data are represented as means ± SEM. Given the paired nature of the experimental design, comparisons between treated groups were made by analysis of variance (ANOVA). A p value <0.05 was considered statistically significant.

References

1 A. Ivask, N. H. Voelcker, S. A. Seabrook, M. Hor, J. K. Kirby, M. Fenech, T. P. Davis and P. C. Ke, *Chem. Res. Toxicol.*, 2015, **28**, 1023–1035.
2 E. A. Proctor, F. Ding and N. V. Dokholyan, *Wiley Interdiscip. Rev. Comput. Mol. Sci.*, 2011, **1**, 80–92.
3 B. R. Brooks, R. E. Bruccoleri, B. D. Olafson, D. J. States, S. Swaminathan and M. Karplus, *J. Comput. Chem.*, 1983, **4**, 187–217.
4 T. Lazaridis and M. Karplus, *Proteins Struct. Funct. Bioinforma.*, 1999, **35**, 133–152.
5 R. P. R. Nanga, J. R. Brender, S. Vivekanandan and A. Ramamoorthy, *Biochim. Biophys. Acta BBA - Biomembr.*, 2011, **1808**, 2337–2342.
6 H. C. Andersen, *J. Chem. Phys.*, 1980, **72**, 2384–2393.
7 G. Schaftenaar and J. H. Noordik, *J. Comput. Aided Mol. Des.*, 2000, **14**, 123–134.
8 J. Wang, R. M. Wolf, J. W. Caldwell, P. A. Kollman and D. A. Case, *J. Comput. Chem.*, 2004, **25**, 1157–1174.
9 A. Hoorens, M. Van de Casteele, G. Klöppel and D. Pipeleers, *J. Clin. Invest.*, 1996, **98**, 1568–1574.
10 I. Kharroubi, L. Ladrière, A. K. Cardozo, Z. Dogusan, M. Cnop and D. L. Eizirik, *Endocrinology*, 2004, **145**, 5087–5096.
11 E. N. Gurzov, F. Ortis, D. A. Cunha, G. Gosset, M. Li, A. K. Cardozo and D. L. Eizirik, *Cell Death Differ*, 2009, **16**, 1539–1550.
12 E. N. Gurzov, J. Barthson, I. Marhfour, F. Ortis, N. Naamane, M. Igoillo-Esteve, C. Gysemans, C. Mathieu, S. Kitajima, P. Marchetti, T. F. Orntoft, L. Bakiri, E. F. Wagner and D. L. Eizirik, *Oncogene*, 2012, **31**, 1723–1732.
13 S. Casas, A. Novials, F. Reimann, R. Gomis and F. M. Gribble, *Diabetologia*, 2008, **51**, 2252–2262.

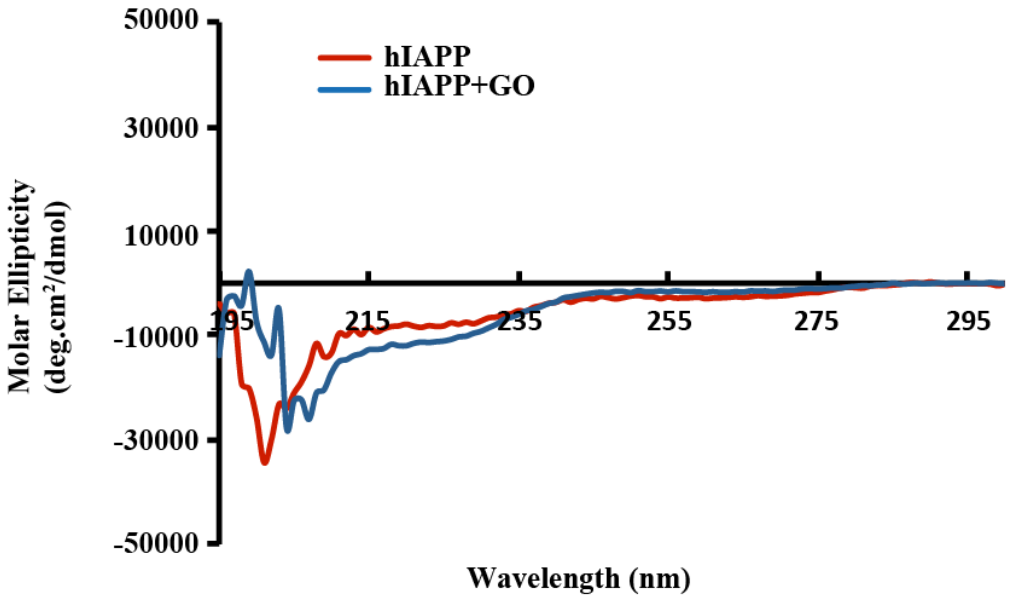

Figure S1. Original circular dichroism (CD) spectra of hIAPP (red, 0.1 mg/mL or 25 μM) and hIAPP mixed with GO (blue, 0.1 mg/mL) of equal volume for 4 h.

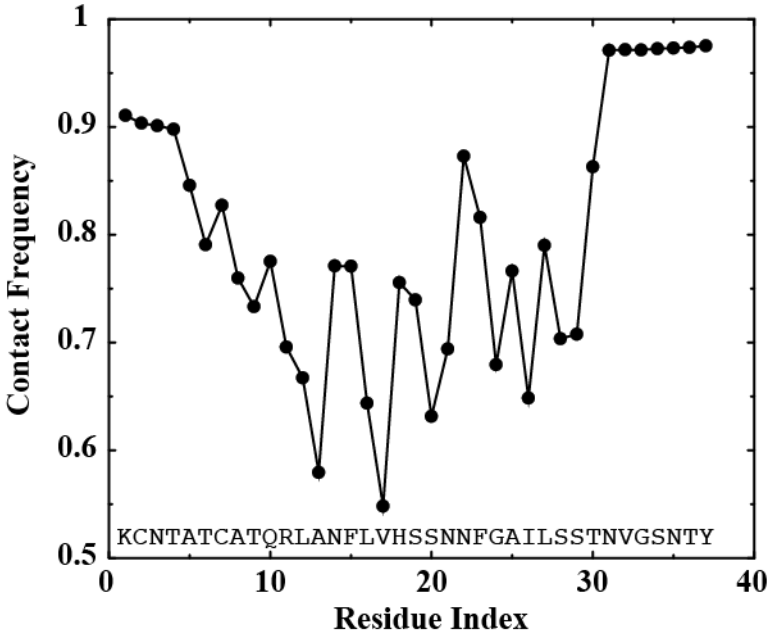

Figure S2. Residue-wise contact frequencies of a single hIAPP with a GO nanosheet. Notably, the binding is dominated by the N- and C-terminal residues and not the hydrophobic residues in the amyloidogenic region. For preparing this plot, we defined a contact between an hIAPP residue and a GO nanosheet if the distance between any two of their atoms was less than or equal to 5Å.

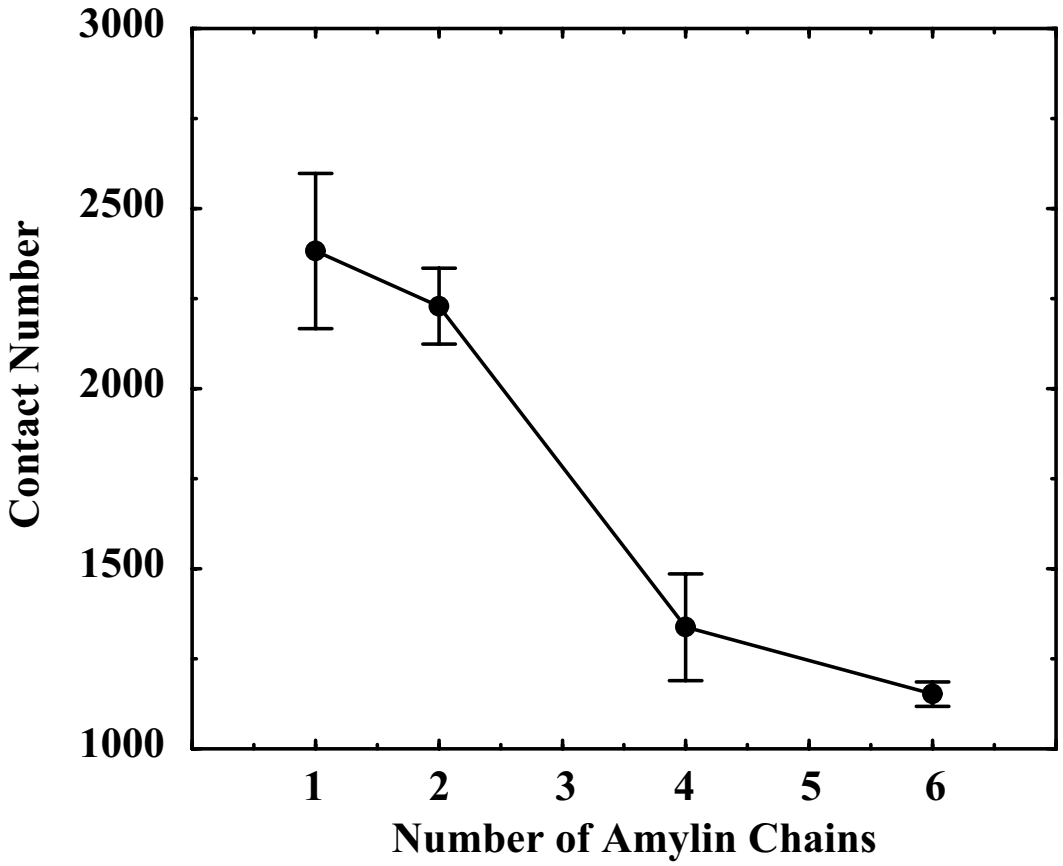

Figure S3. GO-hIAPP contact number per chain as a function of the number of hIAPP chains. As the number of hIAPP chains increase, the per chain contact number decreases.